

Measurement of the $\chi^{(2)}$ tensor of the potassium niobate crystal

Michael V. Pack, Darrell J. Armstrong, and Arlee V. Smith

Department 1118 Lasers, Optics and Remote Sensing, Sandia National Laboratories, Albuquerque, New Mexico 87185-1423

Received January 16, 2003; revised manuscript received May 29, 2003

We use the separated-beams, second-harmonic method to measure the full second-order nonlinear optical tensor of KNbO_3 relative to d_{zxy} of KDP for a fundamental wavelength of 1064 nm. Assuming $d_{zxy}(\text{KDP}) = 0.39$ pm/V, we find for KNbO_3 that $d_{xxx} = 21.9$ pm/V, $d_{xyy} = 8.9$ pm/V, $d_{zzz} = 12.4$ pm/V, $d_{yxy} = 9.2$ pm/V, and $d_{zzx} = 13.0$ pm/V with estimated uncertainties of ± 2 –5%. © 2003 Optical Society of America

OCIS codes: 180.4400, 190.4720.

1. INTRODUCTION

Potassium niobate is a widely used nonlinear crystal. However, there has been some uncertainty about its nonlinear coefficients. Some of the coefficients have been measured multiple times with good agreement on their magnitudes, but with disagreement about their relative signs. For other coefficients, the reported magnitudes are not in good agreement. In addition, violation of Kleinman symmetry is apparent in some measurements. We have measured the full nonlinear tensor in an effort to resolve these issues and to reduce the uncertainty in the nonlinear coefficients.

In the temperature range $-50^\circ\text{C} < T < 223^\circ\text{C}$, KNbO_3 crystals are orthorhombic with point-group symmetry $mm2$. The two-fold rotation axis, or polar axis, is aligned with the principal axis with the lowest refractive index n_x . The form of the nonlinear tensor implied by this crystal symmetry, expressed in the optical frame in which $n_x < n_y < n_z$, is¹

$$\frac{\chi^{(2)}}{2} = d = \begin{bmatrix} d_{xxx} & d_{xyy} & d_{zzz} & 0 & 0 & 0 \\ 0 & 0 & 0 & 0 & 0 & d_{yxy} \\ 0 & 0 & 0 & 0 & d_{zzx} & 0 \end{bmatrix}. \quad (1)$$

Kleinman symmetry adds the further restriction that $d_{xyy} \approx d_{yxy}$ and $d_{zzx} \approx d_{xzz}$. In this paper we present independent measurements of all five tensor coefficients, including their relative signs.

We note that different axis systems are common in other reports, and this is a source of considerable confusion in nonlinear optical applications of KNbO_3 . For the nonlinear crystal user our choice simplifies computations because the linear and nonlinear optical properties are both specified in the same reference frame, which is the standard one for biaxial crystals, namely the frame in which $n_x < n_y < n_z$. Other frames are sometimes used to force the d tensor to have the same form for all class $mm2$ crystals regardless of which principal axis corresponds to the crystallographic two-fold rotation axis of the crystal. In addition the substitution of numbers for the

letter subscripts of the d tensor elements is common. We avoid both of these conventions because they are unnecessary and contribute to the confusion. The form of our d unambiguously indicates that the x axis is the rotation-symmetry axis. To remove any ambiguity in relating d to the underlying crystal structure we note that our x , y , and z axes correspond to the crystallographic axes with lattice spacings of 0.572 nm, 0.569 nm, and 0.370 nm, respectively.²

Previous measurements of these coefficients are summarized in Table 1. Uematsu⁶ measured all five coefficients using a Maker fringe method^{7–9} based on frequency doubling 1064-nm light in two samples, one with entrance and exit faces perpendicular to the y axis, and one with faces perpendicular to the z axis. The coefficients for KNbO_3 were measured relative to d_{zzz} of LiIO_3 which was then related to d_{xxx} of quartz by use of $d_{zzz}(\text{LiIO}_3) = 16.1d_{xxx}(\text{quartz})$. Based on the shapes of the Maker fringes for KNbO_3 , the sign of d_{xyy} was inferred to be opposite that of d_{zzz} and d_{xxx} .

Baumert *et al.*¹⁰ used the wedge variation of the Maker fringe method, also based on frequency doubling 1064-nm light in two KNbO_3 samples, one cut for propagation along the y axis and the other for propagation along the z axis. They measured three coefficients of KNbO_3 relative to d_{xxx} of quartz and found good agreement with Uematsu on the magnitude of the coefficients, as seen in Table 1. However, according to Biaggio *et al.*³ referencing Baumert's Ph.D. thesis,⁴ all of the d 's were found to have the same sign, contradicting Uematsu.

Shoji *et al.*⁵ also used the wedge variation of the Maker fringe method, doubling 1064-nm light in a wedge of KNbO_3 cut for propagation along the y axis. They measured d_{xxx} , d_{xzz} , and d_{zzx} and reported good agreement with Uematsu and Baumert *et al.* on the magnitude of the coefficients; however, they did not comment on the relative signs of the coefficients. It is interesting to note that their quoted uncertainty was smaller than the difference between d_{xzz} and d_{zzx} , indicating a small but significant violation of Kleinman symmetry.

Table 1. Comparison of Measured Values of d_{ijk} Coefficients (in pm/V) for Frequency Doubling 1064-nm Light in KNbO₃

Coefficient	Source of Measurements				
	Uematsu ^a	Baumert ^b	Shoji ^c	Alford ^d	Present Work ^e
d_{xxx}	-18.3	20.5	19.6		21.9±0.5
d_{xyy}	10.6	11.8		7.7±1.0	8.9±0.4
d_{yxy}	11.1	12.4			9.2±0.2
d_{xzz}	-12.0	13.7	10.8		12.4±0.3
d_{zzz}	-11.6	12.8	12.5		13.0±0.4

^aRef. 2 assuming 0.30 pm/V for d_{xxx} of quartz.

^bRef. 3 assuming 0.30 pm/V for d_{xxx} of quartz, signs not reported.

^cRef. 4, absolute measurements, signs not reported.

^dRef. 5, absolute measurement, signs not reported.

^eWe determined that all the d_{ijk} coefficients have the same sign.

Alford and Smith¹¹ used the phase-matched, parametric-amplification process (1064_e nm → 1550_o nm + 3393_o nm) in a crystal cut for propagation in the xz plane to deduce the magnitude of d_{xyy} . They also derived its value based on cw, type I frequency doubling of 982-nm light in a crystal cut for propagation along the z axis, and based on cw, type I frequency doubling of 1319-nm light in a crystal cut for propagation in the xz plane. They published a Miller scaling curve of d_{xyy} versus wavelength for these three processes that indicates the value of d_{xyy} would be 7.7 ± 1.0 pm/V for doubling 1064-nm light. This is substantially smaller than the values of 10.6 pm/V reported by Uematsu and 11.8 pm/V reported by Baumert *et al.*

Other reports of d_{eff} for KNbO₃ include those of Bosenberg and Jarman,¹² Meyn *et al.*,¹³ and Kim and Yoon.¹⁴ Bosenberg and Jarman reported that, based on the oscillation threshold of a 1064-nm pumped KNbO₃ optical-parametric oscillator, the signs of all the d coefficients must be the same, contradicting Uematsu. Meyn *et al.* measured the efficiency of doubling 926-nm light in periodically poled KNbO₃ and concluded that $d_{xyy} \geq 5.8$ pm/V at that wavelength. Kim and Yoon also measured the efficiency of doubling 1064-nm light in quasi-phase-matched KNbO₃ and concluded that $d_{xyy} = 8.2$ pm/V.

2. MEASUREMENT METHOD

In an earlier paper¹⁵ we described a new technique for measuring the full nonlinear tensor. This method, which we call the separated-beams method, permits straightforward measurement of the entire nonlinear tensor, including the relative signs of the coefficients. It is similar in kind to the Maker fringe methods, except the crystal is cut with a large angle on the exit face, as shown in Fig. 1, to disperse the various second-harmonic beams. This greatly simplifies measurement and analysis. If the coherence length of a nonphase-matched, second-harmonic process is short enough that the tilted exit face intersects three or more coherence fringes across the beam diameter, there will be as many as five second-harmonic beams radiated at distinctly different angles. Two of the possible beams can be thought of as generated at the input

face of the crystal and are called the free waves. Their polarizations correspond to the two crystal eigen polarizations, and their exit directions correspond to prism refraction of second-harmonic waves with the refractive indices associated with the two eigen polarizations. If the exit face angle is large enough, these two beams are angularly separated in the far field. The remaining three possible beams, called driven waves, can be thought of as being generated at the exit face of the crystal, and two of them are radiated in directions corresponding to the refractive indices associated with the two fundamental-wave eigen polarizations. The third wave is radiated in the direction corresponding to the average of these two refractive indices, or approximately midway between the other two driven waves. In the Maker fringe methods these waves all overlap, necessitating an elaborate fringe analysis to extract the individual contributions. With the separated-beams method we simply measure the strength of the spatially separated free waves as we rotate the polarization of the input light between its eigen polarizations. A simple analysis yields the various nonlinear tensor elements, including their relative signs.

As we showed in our earlier paper,¹⁵ for propagation along a direction without birefringent walkoff, and in the low-conversion and plane-wave limits, the field of a free wave emitted by a transparent, uncoated crystal is given by

$$E_{\text{free}} = \frac{2d_{\text{eff}} k_0 E_1 E'_1 (\bar{n}_1 + 1)}{\Delta k (n_2 + \bar{n}_1) (n_2 + 1)} t_1 t'_1 t_2 = d_{\text{eff}} E_1 E'_1 \mathcal{N}', \quad (2)$$

where E and E' are the incident fundamental field components along the two orthogonal eigenpolarizations if d_{eff} couples orthogonal fundamental polarizations, or E and E' are both equal to $1/\sqrt{2}$ times the fundamental field component along a single polarization direction if d_{eff} involves a single fundamental polarization. The variable k_0 is the fundamental propagation vector in vacuum, Δk is the phase mismatch ($k_2 - k_1 - k'_1$), n_2 is the refractive index of the free wave, \bar{n}_1 is the mean of the refrac-

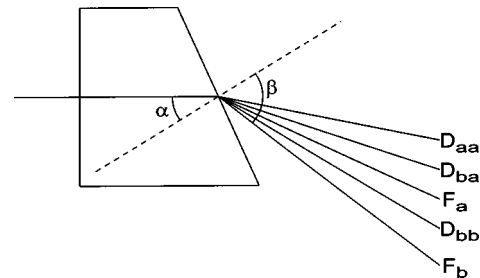


Fig. 1. Diagram of crystal geometry showing the fundamental wave incident normal to left-hand (input) crystal face and the five possible second-harmonic waves refracted at various angles at the right-hand or (exit) crystal face. The dashed line is normal to the output face, and α and β are the incident and refracted angles. The two eigenpolarizations are labeled a and b . The free waves F_b and F_a refract according to $n \sin \alpha = \sin \beta$ with refractive index n equal to $n_b(2\omega)$ and $n_a(2\omega)$, respectively, while the driven waves D_{aa} , D_{ab} , and D_{bb} refract with refractive index n equal to $n_a(\omega)$, $[n_b(\omega) + n_a(\omega)]/2$, and $n_b(\omega)$, respectively. The a - and b -polarized fundamental waves refract in the same direction as D_{aa} and D_{bb} , respectively.

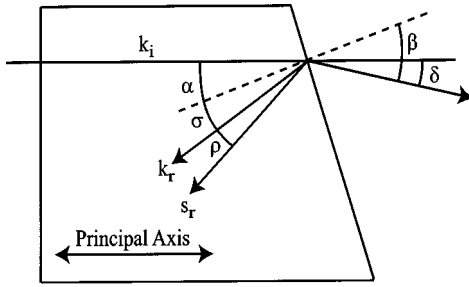


Fig. 2. Diagram of crystal geometry showing the labeling of the angles of the transmitted and reflected waves. The incident fundamental wave and the free and driven harmonic waves propagate along one of the principal axes. A p -polarized wave will reflect at angle σ , which is slightly different from the exit face angle α because of birefringence. For a p -polarized wave the reflected beam also experiences birefringent walk-off indicated by angle ρ . An s -polarized wave reflects at angle α with $\rho = 0$. Angles β and δ are the beam exit angles measured relative to the exit face normal and relative to the original beam direction, respectively.

tive indices n_1 and n'_1 of the two fundamental waves; t_1 and t'_1 are the field transmission coefficients of the fundamental waves at the input face, and t_2 is the field transmission coefficient of the free wave at the exit face. The transmission coefficients are found using

$$t_1 = \frac{2}{1 + n_1}, \quad (3)$$

$$t'_1 = \frac{2}{1 + n'_1}. \quad (4)$$

If the exit face is cut so the eigen polarizations of the free wave correspond to s and p polarizations, the transmission coefficients for the free harmonic waves at the exit face are given by

$$t_2 = \frac{2n_2 \cos \alpha}{n_2 \cos \alpha + \cos \beta} \quad (5)$$

for an s -polarized free wave, and by

$$t_2 = \frac{n_r \cos \alpha \cos \rho + n_2 \cos(\sigma + \rho)}{n_r \cos \beta \cos \rho + \cos(\sigma + \rho)} \quad (6)$$

for a p -polarized free wave where the angles are those shown in Fig. 2. The reflected angle σ is found from

$$n_2 \sin \alpha = n_r \sin \sigma, \quad (7)$$

where n_r is the refractive index of the reflected harmonic wave. The angle ρ is the walk-off angle of the reflected wave. It is the angle between the reflected beam's propagation vector \mathbf{k}_r and Poynting vector \mathbf{S}_r .

We could in principle use Eq. (2) to find d_{eff} by measuring the input and output fields, assuming \mathcal{N} is known. However, in practice we measure pulse energies rather than fields. The pulse energy is proportional to the square of the field multiplied by the beam area, and the beam size changes at the exit face due to inequality of the incidence and exit angles. To account for this we multiply \mathcal{N} by an area correction factor

$$\mathcal{N} = \mathcal{N}' \left(\frac{\cos \beta}{\cos \alpha} \right)^{1/2}. \quad (8)$$

Then we can use

$$U_{\text{free}} = C U_1 U'_1 d_{\text{eff}}^2 \mathcal{N}^2, \quad (9)$$

where C is a constant determined solely by the temporal and spatial profile of the fundamental beam. We use this expression to find relative values of d_{eff} by measuring the relative input and output pulse energies for the sample and reference crystals, assuming we know \mathcal{N} for each. To find \mathcal{N} by using Eqs. (2) and (8) we rely on careful determination of the angles of the exit face and the refraction angles of the free and driven waves. From this we determine the n 's and then calculate \mathcal{N} . Note that if the mixing process involves a single fundamental wave polarized along an eigenpolarization direction, then $U_1 = U'_1$. To keep the notation simple, in this case we artificially divide the fundamental power equally between two beams of the same polarization, which permits us to retain the notation above with no additional degeneracy factors. We note that the area correction term in Eq. (8) was omitted in our earlier paper¹⁵ that introduced the separated-beams method.

Measured values of d_{eff} for a sample crystal can be scaled to those of a reference crystal such as KDP by alternately placing the reference and sample crystals in the same experiment and measuring the relative second-harmonic pulse energies. This eliminates the need for detailed characterization of the fundamental beam's spatial and temporal profiles and for absolute calibration of the input and output pulse energies. We can relate the sample to the reference using

$$d_{\text{eff}} = d_{\text{eff}}(\text{ref}) \left(\frac{E_{\text{free}}}{E_1 E'_1 \mathcal{N}'} \right) \left(\frac{E_1 E'_1 \mathcal{N}}{E_{\text{free}} \mathcal{N}_{\text{ref}}} \right). \quad (10)$$

If we represent the free-pulse energy by \mathcal{F} this can be written

$$d_{\text{eff}} = d_{\text{eff}}(\text{ref}) \frac{\mathcal{N}_{\text{ref}}}{\mathcal{N}} \sqrt{\frac{\mathcal{F}}{\mathcal{F}_{\text{ref}}}}. \quad (11)$$

Our reference was a KDP crystal cut for propagation along the direction $(\theta, \phi) = (90^\circ, 45^\circ)$. We chose KDP as a reference because its nonlinear coefficient has been measured many times with general agreement on the value $d_{zxy} = 0.39 \text{ pm/V}$ for doubling 1064-nm light.^{15,16} This particular cut of KDP has the advantages of no birefringent walk-off and maximum d_{eff} .

3. MEASUREMENTS AND ANALYSIS

Full details of our experimental technique have been published elsewhere.¹⁷ However, we will briefly describe the method and apparatus, which are diagrammed in Fig. 3. The source of our 1064-nm fundamental light is a single-longitudinal-mode Nd:YAG laser producing 9-ns pulses (FWHM). We spatially filter its beam by focusing it through a diamond wire die to provide a beam with a stable, nearly Gaussian spatial profile. A pulse energy of up to 10 mJ is available at the crystal in a beam with a

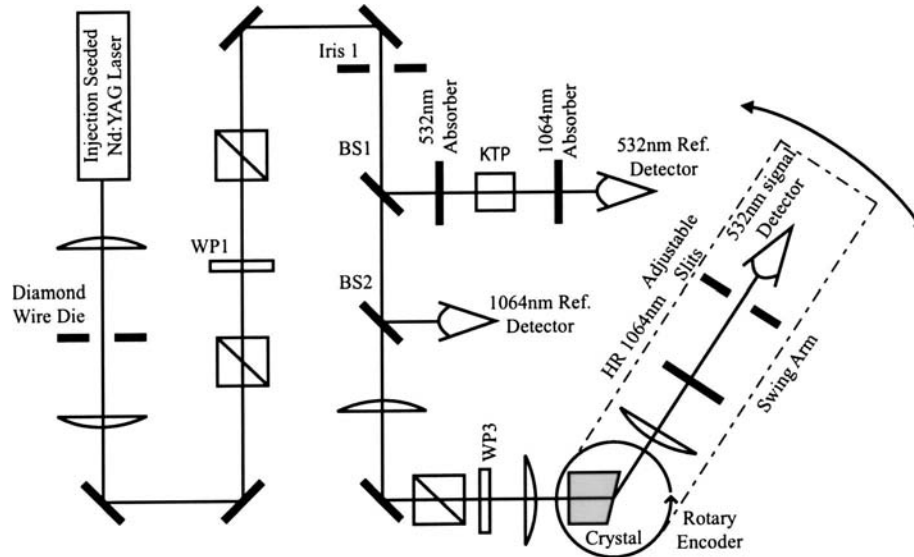


Fig. 3. Diagram of the experimental apparatus. The fundamental pulse energy is adjusted by a half-wave retardation plate (WP1), and the fundamental polarization at the crystal is adjusted by another half-wave plate (WP3). The beam of interest is selected by setting the angle of the swivel arm that carries the 532-nm signal detector. We monitor the fundamental by measuring the 1064-nm energy and by measuring the second harmonic generated in a phase-matched KTP crystal.

Table 2. Multiplier \mathcal{N}_{ijk} and Factors Based on Sellmeier Refractive Indices for KDP with Exit Face Tilted by $\alpha = 19.782^\circ$ and the Face Normal Lying in the yx Plane

Propagation Direction (θ, ϕ)	Polarization	$2k_0/\Delta k$	$t_1 t_1'$	t_2	$\frac{\bar{n}_1 + 1}{(n_2 + 1)(n_2 + \bar{n}_1)}$	$\frac{2k_0(\bar{n}_1 + 1)t_1 t_1' t_2}{\Delta k(n_2 + 1)(n_2 + \bar{n}_1)} \left(\frac{\cos \beta}{\cos \alpha}\right)^{1/2}$ \mathcal{N}_{ijk}
(90°, 45°)	$e(z) - oo$	-42.7	0.6432	1.2292	0.3406	-11.04 ± 0.06

diameter of 1.5 mm ($1/e^2$). A half-wave plate and polarizer provide continuous adjustment of the fundamental pulse energy at the crystal. The crystal is mounted so its input face is normal to the fundamental beam, and the output face is tilted so it refracts the transmitted beams in the plane of the table top. The second-harmonic detector is a photomultiplier mounted on an arm that swivels in the same plane about a point centered on the exit face of the crystal. A focusing lens mounted on the arm just downstream of the crystal focuses the harmonic light on a slit aperture in front of the photomultiplier harmonic detector. The angle of the swing arm is measured to a precision of 0.0001° by a rotary encoder giving the angles β to high precision. The slits provide an angular resolution of about $100 \mu\text{radian}$, or 0.005° . A half-wave plate for 1064-nm light is mounted just before the crystal to allow adjustment of the fundamental polarization at the crystal, and a removable polarizer in front of the photomultiplier verifies the polarization of the second-harmonic beams.

The exit face angles α are measured to a precision of 0.002° by mounting the crystal on a precision rotation stage and measuring the crystal angle when first the input face and then the exit face retroreflect a reference laser beam.

A. Reference KDP Crystal

We measured the KNbO_3 coefficients relative to d_{zxy} of KDP, which has been measured many times and is the *de*

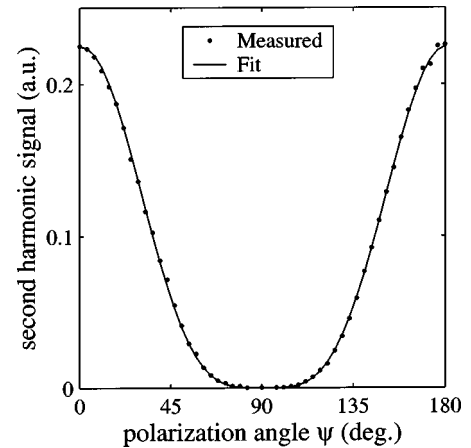


Fig. 4. Relative pulse energy of the z -polarized free harmonic wave from the KDP reference sample as the polarization angle of the linearly polarized fundamental wave is rotated through 180° . At 90° the fundamental is z polarized. The fitted curve has the form of Eq. (13).

facto standard reference. Our reference KDP crystal was cut for propagation along $(\theta, \phi) = (90^\circ, 45^\circ)$ with an exit face angle of $\alpha = 19.782^\circ$. The nonlinear tensor for KDP is

$$d = \begin{bmatrix} 0 & 0 & 0 & d_{xyz} & 0 & 0 \\ 0 & 0 & 0 & 0 & d_{xyz} & 0 \\ 0 & 0 & 0 & 0 & 0 & d_{zxy} \end{bmatrix}. \quad (12)$$

The fundamental wave was polarized in the xy plane and was p polarized at the exit face while the harmonic was z polarized, making $d_{\text{eff}} = d_{zxy}$. The measured refraction angles and refractive indices match the values calculated from the Sellmeier of Ghosh and Bhar.¹⁸ We use the consensus value¹⁶ for d_{zxy} of 0.39 pm/V in deriving the KNbO_3 nonlinearity.

A measurement using only an xy -polarized fundamental would be sufficient for our measurements, but as a check on the cut of the reference crystal and the purity of the fundamental polarization, we rotate the polarization angle of the linearly polarized fundamental 90° either side of the z orientation. The z -polarized free-wave energy should obey

$$\mathcal{F}_z = CU_1^2 |d_{zxy} \mathcal{N}_{zxy} \cos^2 \psi|^2 = A^2 \cos^4(\psi_m + \epsilon), \quad (13)$$

where \mathcal{F}_z is the energy of the z -polarized free wave, U_1 is the full energy of the fundamental pulse, C is a number that depends on the fundamental beam diameter and pulse duration, and ϵ is a small angle representing the difference between the incident fundamental wave polarization angle ψ_m measured relative to the laboratory xy plane and ψ relative to the crystal xy plane. Table 2 lists the parameters used to calculate \mathcal{N}_{zxy} . Figure 4 shows the measured energy as dots and a fit to the data using the form of Eq. (13) as a solid curve. In fitting the data we treat A and ϵ as variables. The value of A in arbitrary units is 0.4747. The same arbitrary unit scale is used for all the KNbO_3 measurements as well.

B. Y-cut KNbO_3 Crystal

We use two KNbO_3 crystals purchased from the company VLOC, Inc., one cut for propagation along the y axis, the other cut for propagation along the z axis. The entrance face for the y -cut crystal is perpendicular to the principal axis \hat{y} , and its exit face is tilted by $\alpha = 20.018^\circ$ with the face normal lying in the yx plane. The expected second-harmonic beams in order of increasing δ angle are \mathcal{D}_{xx} , \mathcal{D}_{xz} , \mathcal{F}_x , \mathcal{D}_{zz} , and \mathcal{F}_z . The free waves have a single subscript indicating the polarization of the harmonic light, while the driven waves have two subscripts because the refraction angle depends on the polarization of both fundamental waves. Measured δ angles of the five second-harmonic beams are listed in Table 3 along with the deduced refractive indices. For comparison we also list in parentheses calculated values for refractive indices based on the Sellmeier equations of Umemura *et al.*¹⁹

From the strength of \mathcal{F}_z when the fundamental is linearly polarized so that $E_x = E_z$, we can find d_{zxx} . From \mathcal{F}_x we can find coefficients d_{xxx} , d_{zzz} in two separate measurements with the fundamental polarized along x or z . The relative signs of d_{xxx} and d_{zzz} can be found by noting the behavior of \mathcal{F}_x as the polarization angle of the fundamental is rotated from x to z . If ψ represents the incident fundamental polarization angle measured from x toward z , the strength of the free wave is given by

$$\begin{aligned} \mathcal{F}_x &= CU_1^2 |d_{zzz} \mathcal{N}_{zzz} \sin^2 \psi + d_{xxx} \mathcal{N}_{xxx} \cos^2 \psi|^2 \\ &= |B \sin^2(\psi_m + \epsilon) + D \cos^2(\psi_m + \epsilon)|^2, \end{aligned} \quad (14)$$

where C is the same number as for the KDP reference. If the products $d_{xxx} \mathcal{N}_{xxx}$ and $d_{zzz} \mathcal{N}_{zzz}$ have opposite signs,

Table 3. Measured Refraction Angles and Refractive Indices^a for KNbO_3

Propagation Axis	Polarization	Exit Face Angle (α)	Free-Wave Angle (δ)	Driven-Wave Angle (δ)	$n_{\text{free}} \equiv n_2$ (Sellmeier) ^b	$n_{\text{driven}} \equiv \bar{n}_1$ (Sellmeier) ^b
z	$x-xx$	20.076°	29.055°	26.595°	2.2035(2.2032)	2.1196(2.1195)
z	$x-yy$	20.076°	29.055°	29.547°	2.2035(2.2032)	2.2198(2.2194)
z	$y-xy$	20.076°	32.785°	28.050°	2.3229(2.3225)	2.1697(2.1695)
y	$x-xx$	20.018°	28.915°	26.465°	2.2030(2.2032)	2.1189(2.1195)
y	$x-zz$	20.018°	28.915°	30.555°	2.2030(2.2032)	2.2570(2.2575)
y	$z-xz$	20.018°	34.565°	28.475°	2.3813(2.3817)	2.1882(2.1885)

^aUsing $n_{\text{air}} = 1.00024$ (corrected for local atmospheric pressure).

^bSellmeier from Umemura.¹⁹

Table 4. Multiplier N_{ijk} and Factors, Calculated from the Measured Refractive Indices for KNbO_3

Propagation Axis	Polarization	$2k_0/\Delta k$	$t_1 t_1'$	t_2	$\frac{\bar{n}_1 + 1}{(n_2 + 1)(n_2 + \bar{n}_1)}$	$\frac{2k_0(\bar{n}_1 + 1)t_1 t_1' t_2}{\Delta k(n_2 + 1)(n_2 + \bar{n}_1)} \left(\frac{\cos \beta}{\cos \alpha}\right)^{1/2} N_{ijk}$
z	$x-xx$	11.91	0.4113	1.738 ^a	0.2253	1.60 ± 0.02
z	$x-yy$	-61.38	0.3860	1.738 ^a	0.2273	-7.81 ± 0.31
z	$y-xy$	6.532	0.3984	1.566	0.2123	0.694 ± 0.006
y	$x-xx$	11.89	0.4113	1.734 ^b	0.2253	1.60 ± 0.02
y	$x-zz$	-18.50	0.3772	1.734 ^b	0.2280	-2.31 ± 0.04
y	$z-xz$	5.179	0.3939	1.588	0.2063	0.525 ± 0.004

^a $\rho = -4.29^\circ$, $\sigma = 19.46^\circ$ (see Fig. 2).

^b $\rho = -2.94^\circ$, $\sigma = 19.59^\circ$ (see Fig. 2).

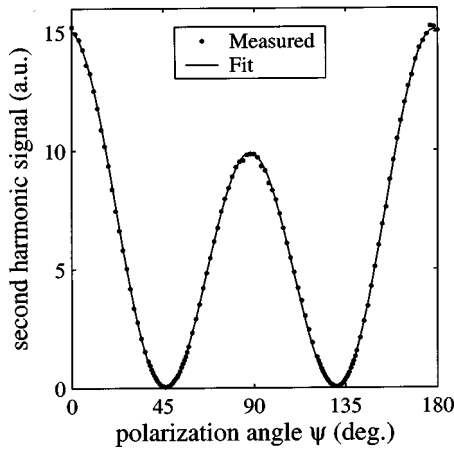


Fig. 5. Relative pulse energy of the x -polarized free harmonic wave from the y -cut KNbO_3 sample as the polarization angle of the linearly polarized fundamental wave is rotated through 180° . At the left and right edges of the graph the fundamental is x polarized and at the center it is z polarized. The fitted curve has the form of Eq. (14).

Table 5. Relative Free-Wave Energies and Derived Values of the d Coefficients of KNbO_3 Assuming d_{zxy} for KDP of 0.39 pm/V

Crystal (Prop. Axis)	Polarization	Best-Fit Parameters	\mathcal{N}_{ijk}	d_{ijk} (pm/V)
KDP	$e(z) - oo$	$A = 0.4747$	-11.04	0.39
$\text{KNbO}_3(z)$	$x-xx$	$S = 3.873$	1.60	21.9 ± 0.5
$\text{KNbO}_3(z)$	$x-yy$	$R = -7.710$	-7.81	8.9 ± 0.4
$\text{KNbO}_3(z)$	$y-xy$	$T = 0.7041$	0.694	9.2 ± 0.2
$\text{KNbO}_3(y)$	$x-xx$	$D = 3.858$	1.60	21.9 ± 0.5
$\text{KNbO}_3(y)$	$x-zz$	$B = -3.153$	-2.31	12.4 ± 0.3
$\text{KNbO}_3(y)$	$z-xz$	$G = 0.7549$	0.525	13.0 ± 0.4

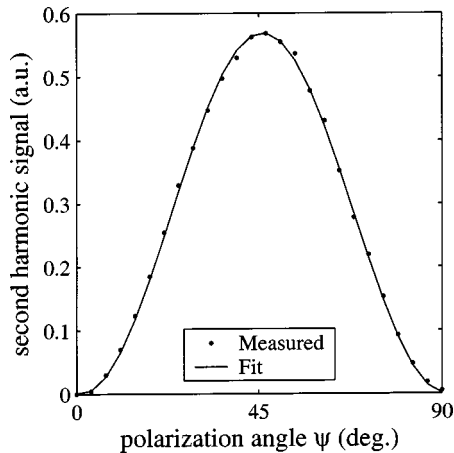


Fig. 6. Relative pulse energy of the z -polarized free harmonic wave from y -cut KNbO_3 as the polarization angle of the linearly polarized fundamental wave is rotated through 90° . At the left the fundamental is x polarized, and at the right it is z polarized. The fitted curve has the form of Eq. (15).

\mathcal{F}_x will have a null lying somewhere between $\psi = 0^\circ$ and $\psi = 90^\circ$, otherwise it will not. Table 4 lists the parameters used to calculate the values of \mathcal{N} for both z -cut and y -cut KNbO_3 crystals. In the case at hand \mathcal{N}_{xxx} and \mathcal{N}_{xzz}

have opposite signs, so the presence of a null would indicate the same signs for d_{xxx} and d_{xzz} while the absence of a null would indicate opposite signs. Figure 5 shows the measured and fitted polarization dependence of \mathcal{F}_z . The fit parameters B and D are listed in Table 5.

The polarization dependence of the z -polarized free wave \mathcal{F}_z is given by

$$\begin{aligned} \mathcal{F}_z &= CU_1^2 |d_{zxx} \mathcal{N}_{zxx} \sin(2\psi)|^2 \\ &= G^2 \sin^2(2\psi_m + \epsilon). \end{aligned} \quad (15)$$

Figure 6 shows the measured and fitted curves of \mathcal{F}_z , and the fit parameter G is listed in Table 5. The excellence of the fit verifies that there were no accidental contributions from any of the other harmonic beams due to either light scatter or by having the detector slits spaced too far apart.

The value of d_{xxx} is found by using

$$\begin{aligned} d_{xxx} &= d_{\text{ref}} \frac{\mathcal{N}_{\text{ref}} D}{\mathcal{N}_{xxx} A} = 0.39 \frac{(11.04)}{(1.597)} \frac{(3.858)}{(0.4747)} \\ &= 21.9 \text{ pm/V}. \end{aligned} \quad (16)$$

In comparing the other KNbO_3 and KDP curve-fitting coefficients and values of \mathcal{N} we find $d_{xzz} = 12.4 \pm 0.35 \text{ pm/V}$ and $d_{zxx} = 13.0 \pm 0.45 \text{ pm/V}$. The sign of d_{zxx} relative to d_{xxx} and d_{xzz} is not determined from these measurements, but according to Kleinman symmetry $d_{zxx} \approx d_{xzz}$, so it seems safe to assume that d_{zxx} and d_{xzz} must have the same sign.

C. Z-cut KNbO_3 Crystal

This measurement is similar to that of the y -cut crystal except the z polarization is replaced by the y polarization. The crystal is cut for propagation along the z axis with the entrance face perpendicular to z , and the exit face is tilted by $\alpha = 20.076^\circ$ with its face normal lying in the zx plane. This crystal is used to measure d_{xxx} , d_{xyy} , and d_{yxy} . The polarization dependence of \mathcal{F}_x is given by

$$\begin{aligned} \mathcal{F}_x &= CU_1^2 |d_{xyy} \mathcal{N}_{xyy} \sin^2 \psi + d_{xxx} \mathcal{N}_{xxx} \cos^2 \psi|^2 \\ &= |R \sin^2(\psi_m + \epsilon) + S \cos^2(\psi_m + \epsilon)|^2. \end{aligned} \quad (17)$$

Figure 7 shows the measured and fitted curves of \mathcal{F}_x , and the fit parameters R and S are listed in Table 5.

The polarization dependence of the y -polarized free wave \mathcal{F}_y is given by

$$\begin{aligned} \mathcal{F}_y &= CU_1^2 |d_{yxy} \mathcal{N}_{yxy} \sin(2\psi)|^2 \\ &= T^2 \sin^2(2\psi_m + \epsilon). \end{aligned} \quad (18)$$

Figure 8 shows the measured and fitted curves of \mathcal{F}_z ; the fit parameter G is listed in Table 5.

In comparing the KNbO_3 and KDP pulse energies, we find $d_{xxx} = 21.9 \pm 0.45 \text{ pm/V}$, $d_{xyy} = 8.9 \pm 0.45 \text{ pm/V}$, and $d_{yxy} = 9.2 \pm 0.2 \text{ pm/V}$. The signs of d_{xxx} and d_{xyy} are the same because there is a null in \mathcal{F}_x , and the signs of \mathcal{N}_{xxx} and \mathcal{N}_{xyy} are opposite. The sign of d_{yxy} relative to d_{xxx} and d_{xyy} is not determined from these measurements, but according to Kleinman symmetry $d_{yxy} \approx d_{xyy}$, so d_{yxy} and d_{xyy} should have the same sign.

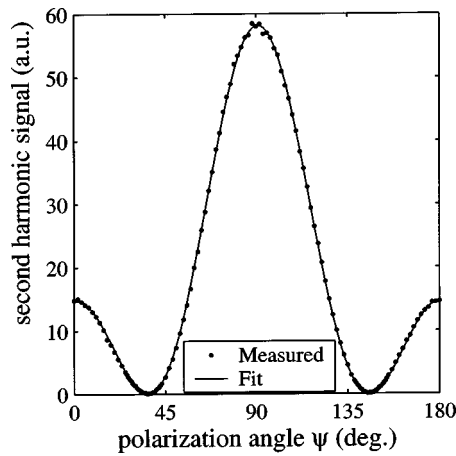


Fig. 7. Relative pulse energy of the x -polarized free harmonic wave from z -cut KNbO_3 as the polarization angle of the linearly polarized fundamental wave is rotated through 180° . At the left and right edges of the graph the fundamental is x polarized, and at the center it is y polarized. The fitted curve has the form of Eq. (17).

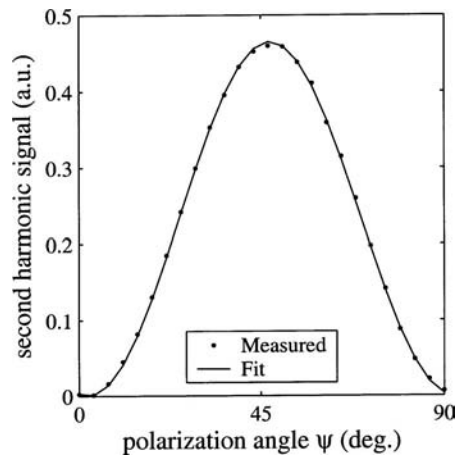


Fig. 8. Relative pulse energy of the y -polarized free harmonic wave from z -cut KNbO_3 as the polarization angle of the linearly polarized fundamental wave is rotated through 90° . At the left edge of the graph the fundamental is x polarized, and at the right it is y polarized. The fitted curve has the form of Eq. (18).

4. CONCLUSIONS

We have used the separated-beams method to compare accurately each of the tensor elements of KNbO_3 with d_{xyz} of KDP. Our results are summarized in Table 1. We conclusively demonstrate that the signs of all coefficients are the same, and we find that Kleinman symmetry holds within our experimental accuracy for both $d_{xzz} \approx d_{zzx}$ and $d_{xyy} \approx d_{yyx}$. Our coefficients are in good agreement with previous measurements, and we believe our claim of ± 2 –5% overall accuracy is a realistic estimate of the total uncertainty in our measurements. Coefficient d_{xxx} was measured independently using the y -cut and the z -cut samples, and the two values agreed to well within our quoted uncertainty. The principal contribution to the uncertainty is usually from the uncertainty in Δk , one of the terms in \mathcal{N} . Its uncertainty is relatively large because it is proportional to a small difference in refractive indices. In our measurements the uncertainty in Δk is always 4% or less. Most of the remaining uncer-

tainty arises from a small amount of shot noise at the detector and slight variations in the laser pulses.

ACKNOWLEDGMENT

Sandia is a multiprogram laboratory operated by Sandia Corporation, a Lockheed Martin Company, for the United States Department of Energy's National Nuclear Security Administration under contract DE-AC04-94AL85000.

Corresponding author A. V. Smith may be reached by e-mail at arlsmit@sandia.gov.

REFERENCES AND NOTES

1. R. W. Boyd, *Nonlinear Optics* (Academic, New York, 1999).
2. B. Zysset, I. Biaggio, and P. Gunter, "Refractive indices of orthorhombic KNbO_3 . I. Dispersion and temperature dependence," *J. Opt. Soc. Am. B* **9**, 380–386 (1992). Our x-ray diffraction measurements confirm that the z -axis lattice spacing is 0.370 nm and that the x - and y -axis lattice spacings are both approximately 0.57 nm, but our resolution was not sufficient to differentiate between the x - and y -axis lattice spacings.
3. I. Biaggio, P. Kerkoc, L.-S. Wu, P. Guenter, and B. Zysset, "Refractive indices of orthorhombic KNbO_3 . II. Phase-matching configurations for nonlinear optical interactions," *J. Opt. Soc. Am. B* **9**, 507–517 (1992).
4. J.-C. Baumert, "Nichtlineare optische Eigenschaften und Anwendungen von KNbO_3 Kristallen," Ph.D. dissertation ETH 7802 (Swiss Federal Institute of Technology, Zurich, Switzerland, 1985).
5. I. Shoji, T. Kondo, A. Kitamoto, M. Shirane, and R. Ito, "Absolute scale of second-order nonlinear optical coefficients," *J. Opt. Soc. Am. B* **14**, 2268–2294 (1997).
6. Y. Uematsu, "Nonlinear optical properties of KNbO_3 single crystal in the orthorhombic phase," *Jpn. J. Appl. Phys.* **13**, 1362–1368 (1974).
7. P. D. Maker, R. W. Terhune, M. Nisenoff, and C. M. Savage, "Effects of dispersion and focusing on the production of optical harmonics," *Phys. Rev. Lett.* **8**, 21–22 (1962).
8. J. Jerphagnon and S. K. Kurtz, "Maker fringes: a detailed comparison of theory and experiment for isotropic and uniaxial crystals," *J. Appl. Phys.* **41**, 1667–1681 (1970).
9. W. N. Herman and L. M. Hayden, "Maker fringes revisited: second-harmonic generation from birefringent or absorbing materials," *J. Opt. Soc. Am. B* **12**, 416–427 (1995).
10. J.-C. Baumert, J. Hoffnagle, and P. Guenter, "Nonlinear optical effects in KNbO_3 crystals at $\text{Al}_x\text{Ga}_{1-x}\text{As}$, dye, ruby, and Nd:YAG laser wavelengths," *1984 European Conference on Optics, Optical Systems, and Applications*, B. Bolger and H. A. Ferwerda, eds., Proc. SPIE **492**, 374–385 (1984).
11. W. J. Alford and A. V. Smith, "Wavelength variation of the second-order nonlinear coefficients of KNbO_3 , KTiOPO_4 , KTiOAsO_4 , LiNbO_3 , LiIO_3 , $\beta\text{-BaB}_2\text{O}_4$, KH_2PO_4 , and LiB_3O_5 crystals: a test of Miller wavelength scaling," *J. Opt. Soc. Am. B* **18**, 524–533 (2001).
12. W. R. Bosenberg and R. H. Jarman, "Type-II phase-matched KNbO_3 optical-parametric oscillator," *Opt. Lett.* **18**, 1323–1325 (1993).
13. J.-P. Meyn, M. E. Klein, D. Woll, R. Wallenstein, and D. Rytz, "Periodically poled potassium niobate for second-harmonic generation at 463 nm," *Opt. Lett.* **24**, 1154–1156 (1999).
14. J. H. Kim and C. S. Yoon, "Domain switching characteristics and fabrication of periodically poled potassium niobate for second-harmonic generation," *Appl. Phys. Lett.* **81**, 3332–3334 (2002).
15. R. J. Gehr and A. V. Smith, "Separated-beam, nonphase-matched, second-harmonic method of characterizing nonlinear optical crystals," *J. Opt. Soc. Am. B* **15**, 2298–2307 (1998).

16. D. A. Roberts, "Simplified characterization of uniaxial and biaxial nonlinear optical crystals: a plea for standardization of nomenclature and conventions," *IEEE J. Quantum Electron.* **28**, 2057–2074 (1992).
17. D. J. Armstrong, M. V. Pack, and A. V. Smith, "Instrument and method for measuring second-order nonlinear optical tensors," *Rev. Sci. Instrum.* **74**, 3250–3257 (2003).
18. G. C. Ghosh and G. C. Bhar, "Temperature dispersion in ADP, KDP, and KD*P for nonlinear devices," *IEEE J. Quantum Electron.* **QE-18**, 143–145 (1982).
19. N. Umemura, K. Yoshida, and K. Kato, "Phase-matching properties of KNbO₃ in the mid-infrared," *Appl. Opt.* **38**, 991–994 (1999).